Published in final edited form as:
Int J Radiat Oncol Biol Phys. 2012 July 15; 83(4): 1132–1140. doi:10.1016/j.ijrobp.2011.09.045.

Accumulated Dose in Liver Stereotactic-Body Radiotherapy: Positioning, Breathing and Deformation Effects

Michael Velec, B.Sc.[1], **Joanne L. Moseley, B.Math.**[1], **Tim Craig, Ph.D.**[1,2], **Laura A. Dawson, M.D.**[1,2], and **Kristy K. Brock, Ph.D.**[1,2,3]

[1]Radiation Medicine Program, Princess Margaret Hospital, University Health Network, Toronto, Canada

[2]Department of Radiation Oncology, University of Toronto, Toronto, Canada

[3]Department of Medical Biophysics, University of Toronto, Toronto, Canada

Abstract

Purpose—To investigate the accumulated dose deviations to tumors and normal tissues in liver stereotactic-body radiotherapy (SBRT), and investigate their geometric causes.

Methods and Materials—Thirty previously treated liver cancer patients were retrospectively evaluated. SBRT was planned on the static exhale CT for 27 – 60 Gy in 6 fractions, and patients were treated in free-breathing with daily cone-beam CT (CBCT) guidance. Biomechanical model-based deformable image registration accumulated dose over both the planning 4DCT (predicted breathing dose), and also over each fraction's respiratory-correlated CBCT (accumulated treatment dose). The contribution of different geometric errors on changes between the accumulated and predicted breathing dose were quantified.

Results—Twenty one patients (70%) had accumulated dose deviations relative to the *planned static prescription dose* greater than 5%, ranging from −15 to 5% in tumors and −42 to 8% in normal tissues. Sixteen patients (53%) still had deviations relative to the *4DCT-predicted dose*, which were similar in magnitude. Thirty two tissues in these 16 patients had deviations > 5% relative to the 4DCT-predicted dose, and residual setup errors (n=17) were most often the largest cause of the deviations, followed by deformations (n=8) and breathing variations (n=7).

Conclusion—The majority of patients had accumulated dose deviations greater than 5% relative to the static plan. Significant deviations relative to the predicted breathing dose still occurred in over half the patients, commonly due to residual setup errors. Accumulated SBRT dose may be warranted to pursue further dose-escalation, adaptive SBRT, and aid in correlation with clinical outcomes.

Corresponding Author Info: Michael Velec, MRT(T), Radiation Medicine Program, Princess Margaret Hospital, 610 University Ave., Toronto, Ontario, Canada, M5G 2M9. Tel: (416) 946-4501; Fax (416) 946-6566; michael.velec@rmp.uhn.on.ca.

Presented in part at the 51st Annual Meeting of the American Society for Radiation Oncology (ASTRO), Chicago, IL, November 1–5, 2009.

Conflict of Interest Notification

Dr. Brock serves on the IMPAC Physics Advisory Board and receives grant funding from Philips Medical Systems, RaySearch Laboratories and Elekta Oncology Systems. Dr. Dawson receives grant funding from Bayer. Drs. Brock and Dawson have financial interest in the Morfeus technologies reported.

Keywords

Deformable registration; Dose accumulation; Image-guided radiotherapy; Stereotactic-body radiotherapy; Liver cancer

Introduction

Stereotactic-body radiotherapy (SBRT) is a promising treatment for primary and metastatic liver cancer patients ineligible for other localized treatment. SBRT planning uses individualized, highly conformal dose distributions aimed at reducing treatment margins and sparing normal tissue dose and related toxicity. Liver normal tissue complication probability (NTCP) models can help estimate SBRT toxicity and allocate or escalate dose (1, 2). Trials have shown high local control rates with acceptable toxicity(3–5), while lower doses have been associated with poorer survival or disease control(1, 4), suggesting further dose escalation may be beneficial provided toxicity rates remain low.

Minimizing geometric uncertainties is necessary for SBRT. Respiratory motion can be negated using active breathing control (ABC) devices allowing gated beam delivery during breath holds(6), or reduced with an abdominal compression plate(7). These may allow for smaller margins, normal tissue sparing and higher tumor doses, but many patients are ineligible and are treated in free-breathing. Incorporating breathing motion into liver SBRT dose calculations can potentially impact tumor and normal tissue doses, and margin design(8–10). Whether these techniques actually estimate the delivered dose better than static dose calculations is presently unknown. Image-guided radiotherapy (IGRT) can potentially identify and correct baseline shifts in liver position (relative to bone), breathing motion or deformation prior to treatment (6, 11, 12). Direct tumor visualization is typically not possible so IGRT methods for liver SBRT involve imaging fiducial markers(13) or the liver and diaphragm as soft-tissue surrogates using 2D fluoroscopy or 3D cone-beam CT (CBCT), in the presence of breathing motion (7, 14).

Romero *et al.* (15) estimated daily dose deviations in a liver SBRT trial using rigidly-registered repeat CT, finding IGRT did not on average improve the daily dose to normal tissues due to anatomical deformations. Rigid registration is unable to accumulate dose over multiple fractions, in the presence of these changes. Deformable image registration (DIR) applies spatially variable transformations during registration to more accurately track tissues between two or more imaging sessions (i.e. SBRT fractions). Janssens *et al.* (16) found intensity-based DIR significantly improved interfraction dose accumulation on deforming phantoms over rigid registration, noting its accuracy is highly dependent on both image quality and contrast. They also reported that sharp dose gradients, required by liver SBRT plans to spare normal tissue, can exacerbate dose accumulation errors caused by DIR errors. Soft-tissue contrast is generally poor on CBCT making IGRT and DIR challenging. Brock *et al.* (11) applied a biomechanical model-based DIR algorithm on the daily CBCT of liver SBRT patients, revealing residual errors in the tumor position that exceeded the setup tolerance in 15% of fractions. The dosimetric impact of these uncertainties is not well understood.

Our previous work, Velec, *et. al.*(9), indicated that performing deformable dose accumulation incorporating breathing motion from the 4D CT resulted in substantial deviations in the estimated dose to the tumor and normal tissues compared to the static plan. The work presented here expands on this, evaluating how well the planning 4D CT predicts for the best estimate of delivered dose, using deformable dose accumulation over each fraction's 4D CBCT. The aim was to accumulate dose using DIR of CBCT over 6-fraction

SBRT, in free-breathing liver patients. This was compared to both the static dose on the planning CT, and the breathing dose predicted from the planning 4D CT, to assess which method better predicts the accumulated dose. The second aim was to investigate the effect of different geometric uncertainties on dose deviations. Characterizing uncertainties in current SBRT techniques may enable robust planning development, enable safe escalation of SBRT doses in future trials, and improve interpretation of clinical outcomes.

Methods and Materials

Patients and SBRT planning

Thirty patients previously treated on institutional review board-approved phase I and II trials of dose escalated, hypofractionated liver SBRT from February 2006 to April 2010 were investigated. Patient and planning details are summarized in Table 1. All were ineligible for ABC breath-hold treatment due to intolerance or small breathing amplitudes (<5 mm), thus were treated in free-breathing (±abdominal compression). Planning was done on end-exhale 4D CT. Inhale 4D CT liver motion, diaphragm fluoroscopy motion and cine-MRI tumor motion, aided in breathing motion characterization for designing individualized planning target volumes (PTV). Delineation and static plan optimization was done on exhale CT in a commercial treatment planning system (Pinnacle^3 v7.6 – 8.0, Philips Medical Systems, Madison WI). Asymmetric PTVs were designed to account for the patient-specific breathing motion observed on the imaging studies, with a minimum PTV of 5 mm required. Dose was individually prescribed for 6 fractions in 2 weeks by determining the risk of radiation-inducted liver disease from a Lyman-NTCP model(2). The primary planning goal was that the minimum dose to the GTV and PTV received a minimum of 95% of the prescribed dose to 0.5 cc, while respecting normal tissue constraints. The maximum allowable doses to the luminal gastrointestinal organs ranged from 30 to 36 Gy to 0.5 cc. Volume, margin generation, and NTCP calculations have been detailed by Dawson *et al.* (2).

IGRT

Patients were treated with daily IGRT in free-breathing on linacs equipped with kV CBCT and fluoroscopy (Synergy, Elekta AB, Stockholm, Sweden). Prior to treatment, anterior-posterior fluoroscopy was acquired to assess the maximum exhale diaphragm position and breathing amplitude compared to the planning images. In addition, a 360° CBCT was acquired and rigidly registered to the planning exhale CT using a 3D liver-liver alignment. Breathing artifacts blurred the CBCT, therefore the liver match was biased to the superior part of the blur, closer to planned exhale CT position. This soft-tissue IGRT strategy accounted for baseline liver shifts relative to bony anatomy. Tolerance for image registration was 3 mm and 5°, and any corrections were verified with repeat imaging.

For offline research analysis, a CBCT was acquired in the final treatment position prior to SBRT. These were retrospectively sorted into ten respiratory-correlated phases (4D CBCT) (17), and the end-exhale and end-inhale phases were extracted.

Deformable image registration and dose accumulation

Dose accumulation requires that tissues be accurately tracked between images. DIR has more degrees of freedom over rigid registration to realistically map soft tissue motion and deformation. This study used Morfeus, a multi-organ biomechanical model-based DIR algorithm, previously described in detail (18). Briefly, a base model is first created by converting the exhale CT planning contours into 3D surface meshes and filled with tetrahedral elements. The liver, external body and spleen meshes are deformed into their corresponding secondary surface meshes, created from additional contouring (by M.V.) on secondary images (e.g. inhale CT, CBCT etc.) via guided surface projections (HyperMorph,

Altair Engineering, Troy MI). All elements, including GTV and organs without secondary contours, are implicitly deformed by tissue biomechanics and solved using finite element analysis (Fig. 1). The ability of Morfeus to accurately track the entire volume of the organs of interest (i.e. the liver, including the interior volume) has been previously quantified using visible anatomical landmarks within the liver. This accuracy is 2 mm (18).

For this study, dose was accumulated and compared in the Morfeus environment. The static clinical plan was calculated on both the exhale and inhale planning CT in the treatment planning system, providing two extreme dose matrices occurring during breathing, and imported into Morfeus. DIR provides the location of all elements in the model between exhale and inhale images on 4D CT or 4D CBCT. To accumulate a breathing dose, the dose matrices are interpolated onto each element's position at exhale, inhale, and four linearly-interpolated intermediate phases. Each phases' contribution is weighted according to the element's position in the breathing cycle, as well as time spent in that phase(19). Element dose was summed across the breathing cycle as reported by Velec *et al.* (9).

Three doses were calculated:

Planned dose (D_{plan}) is the static clinical plan, replicated by interpolating the exhale CT dose matrix onto the initial mesh model at exhale CT. No breathing motion, setup errors, deformation or dose accumulation is considered.

Predicted dose (D_{pred}) is the breathing dose predicted by the planning 4D CT. Exhale CT is deformed to inhale CT. The exhale and inhale CT dose matrices are interpolated onto this deformation map to accumulate breathing dose. Interfraction setup errors, deformations, and breathing *changes* over the course of SBRT are not considered.

Accumulated dose (D_{acc}) is the dose accumulated over the course of SBRT. Exhale CT is first deformed to each fraction's exhale CBCT, to account for all baseline interfraction changes (setup errors, baseline liver shifts, deformation etc.) and subsequently deformed to each inhale CBCT to account for the daily breathing motion. The exhale and inhale CT dose matrices are interpolated onto each fraction's exhale to inhale CBCT deformation map to accumulate breathing dose, and subsequently the doses from all 6 fractions are then summed. Note that daily dose matrices were not recalculated using each CBCT, to avoid the CBCT-number inaccuracies. Rather, DIR was used to track anatomical motion and deformation within the dose matrices calculated on the initial planning 4D CT, and accumulate the dose therein.

D_{acc} was primarily compared to D_{pred} for reporting changes in accumulated dose (D_{acc}–D_{pred}), as the clinical plans did not model breathing motion. However, differences between the accumulated and planned static doses (D_{acc}–D_{plan}) were also computed to investigate whether 4D calculations (D_{pred}) are superior in predicting D_{acc} than D_{plan}. Minimum dose (to 0.5 cc) to GTV(s), mean dose to liver and kidneys, and maximum dose (to 0.5 cc) to all other organs were investigated. Dose deviations are described as a percent of the prescribed dose, and large deviations (≥ 5%) are assumed to be potentially clinically significant. Liver NTCP changes were also investigated.

Rigid geometric uncertainties during treatment were calculated for each tissue's centre-of-mass (COM) displacement as the group mean (M), systematic (Σ_{COM}) and random (σ_{COM}) errors (20). Deformation geometric uncertainties were calculated using van Mourik's method (21), with the liver COM subtracted from each tissue prior to calculating the group systematic (Σ_{DEF}) and random (σ_{DEF}) errors. Errors were calculated between the planned position on exhale CT and daily exhale CBCT (which accounts for baseline liver shifts

relative to vertebral bodies), and between exhale and inhale CBCT. Results are in the left-right (LR), anterior-posterior (AP) and superior-inferior (SI) directions.

Comparison of geometric uncertainties

Identification of the cause of dose deviations was a secondary study aim. All deformable registrations started from exhale CT, preserving the number and sequencing of elements in the base model. This facilitated tracking and dose accumulation, and allowed the displacement map from one registration (exhale CT to inhale CT) to be applied to the results of another registration (exhale CT deformed exhale CBCT). This feature was exploited to investigate the relative importance of different geometric errors on dose deviations (D_{acc}–D_{pred}) by comparing several scenarios (Fig. 2):

Breathing Variations—These are changes in breathing motion and breathing deformation between planning (4D CT) and treatment (4D CBCT). D_{acc} (Fig. 2B) was compared to a modified accumulation (Fig. 2C) that deforms exhale CT to exhale CBCT (identical to D_{acc}) to account for all interfraction changes, but subsequently applies the predicted 4D CT deformation map (not the 4D CBCT deformation map). Both scenarios identically model interfraction errors (setup, baseline shifts, and deformation etc.) allowing the effect of breathing changes on dose accumulation to be measured.

Residual Setup—These are positioning errors, or the rigid liver COM differences between exhale CT and exhale CBCT. D_{pred} (Fig. 2A) was compared to a modified accumulation (Fig. 2D) that accounts for daily setup errors using rigid liver registration between exhale CT and exhale CBCT (not deformable registration as in D_{acc}), and subsequently applies the predicted 4D CT deformation map (identical to D_{pred}). Each scenario modeled breathing identically, whereas the latter accounts for residual setup effects in the dose accumulation. Other interfraction changes (baseline liver shifts, deformation etc.) are not modeled in this comparison.

Deformations—This is abdominal deformation. It includes baseline differences in tissue position (relative to liver) and shape changes of all tissues between exhale CT and exhale CBCT. Two modified accumulations scenarios were compared. The first (Fig. 2C) accounts for interfraction changes between exhale CT and exhale CBCT using DIR (setup errors, baseline shifts, deformation), while the second (Fig. 2D) uses rigid liver COM registration (ignoring baseline shifts and deformation). Both scenarios subsequently apply the predicted 4D CT deformation map to model breathing motion. Therefore, accounting for interfraction changes with either deformable or rigid registration is measured.

Results

Dose was accumulated for thirty patients at planning (D_{pred}) and over the entire treatment course (D_{acc}), using DIR of 60 4D CT and 360 4D CBCT images respectively.

Geometric uncertainties

Group geometric uncertainties evaluated after DIR are summarized in Table 2. Between exhale CT and exhale CBCT, nine patients (30%) had individual systematic (mean) residual GTV COM errors > 3 mm in any direction. These occurred in the LR, AP and SI directions in 2, 6 and 5 patients respectively, up to a maximum of 11 mm. Sixteen patients (53%) had three or more fractions with residual GTV COM errors > 3 mm. Between 4D CBCT and 4D CT, sixteen patients (53%) had mean changes in the GTV COM breathing magnitude of at least 3 mm in any direction,. These changes of −11 to 8 mm occurred in LR, AP and SI

directions in 2, 6 and 12 patients respectively. Sixteen patients (53%) had at least 3 fractions with changes in GTV COM breathing motion > 3 mm.

Accumulated dose changes

Accumulated dose is compared to the planned and predicted dose in Table 3. Relative to the planned dose (D_{acc}–D_{plan}), 21 patients (70%) had large dose deviations ($|\Delta| \geq 5\%$) to any tissue or GTV. Thirty nine tissues in these 21 patients had deviations, and 34 (87%) of these were dose decreases compared to D_{plan}. Relative to the predicted dose (D_{acc}–D_{pred}), 16 patients (53%) had large dose changes to any tissue or GTV. Thirty two tissues in these 16 patients had significant changes, with 55% decreasing and 45% increasing in dose compared to D_{pred}. Mean accumulated dose (D_{acc}) differed significantly ($p<0.05$) from the planned dose (D_{plan}) for the majority of organs. Mean accumulated deviations relative to the predicted dose (D_{acc}–D_{pred}) differed significantly, and were often smaller in magnitude, from mean deviations relative to the static plan (D_{acc}–D_{plan}). This suggests D_{pred} may be better overall at predicting the accumulated dose, particularly for the normal gastrointestinal organs, however a large range of deviations were still observed. An example of dose deviations relative to both the planned and predicted dose is shown in Figure 3.

The contribution of each geometric error on deviations from the predicted dose (D_{acc}–D_{pred}) is shown in Figure 4 for selected critical organs. For the 32 tissues that did have large deviations, residual setup errors were the largest cause in 17 tissues (effect size: −15 to 18%), deformation in 8 tissues (effect size: −22 to 11%), and breathing variations in 7 tissues (effect size: −9 to 7%). Although many tissues had small overall dose deviations < 5%, geometric errors were individually observed to have large effects that could offset each other (see Figure 4).

Three patients had significant GTV dose deviations (D_{acc}–D_{pred}). One patient with three GTVs had an increase of 5% to a portal-vein thrombus being treated to a lower dose than the other GTVs. This thrombus had residual systematic errors of 5 mm left and 10 mm posterior, shifting it towards the other higher dose GTVs. Another patient had a GTV dose increase of 13% relative to D_{pred} (see Figure 3). The third patient with a decrease in minimum GTV dose of 14% due to deformation is shown in Figure 5.

Liver NTCP changes after accumulation were small as the initial planned NTCP was often low (<2%), and mean liver dose deviations (D_{acc}–D_{pred}) were small. Two patients had NTCP increases relative to D_{pred} of 8.8% and 9.4%, caused by 3 mm residual systematic setup errors and 8 mm less superior-inferior mean breathing motion respectively. These errors moved more normal liver into the high dose region.

Discussion

Accumulated dose was investigated for thirty liver SBRT patients. This is the first study using DIR of daily 4D CBCT to accumulate dose over the entire course of 6-fraction liver SBRT, simultaneously accounting for and evaluating the relative importance of different geometric uncertainties. Significant accumulated dose deviations relative to either the planned distribution (D_{acc}–D_{plan}), or the breathing dose distribution modeled with the planning 4D CT (D_{acc}–D_{pred}), were observed in the majority of patients. Residual setup errors, observed after DIR of 4D CBCT, followed by deformation and breathing variations, were the most common source of deviations.

This study compared D_{acc} to the static plan on exhale CT (D_{plan}) and to the planning 4D CT-predicted breathing dose (D_{pred}) to help determine which distribution is more representative of the actual delivered dose. Overall, the mean changes between D_{acc} and D_{pred} significantly

differed, and were often smaller in magnitude, compared to changes between D_{acc} and D_{plan} (Table 3). 4D breathing dose distributions (D_{pred}) may be more robust than static distributions (D_{plan}) particularly for the duodenum and bowels, often dose-limiting at planning(9).

In the clinical trials that these patients were treated on, the prescribed dose was limited by the liver NTCP or other normal tissue doses on D_{plan}, which were more often lower after accumulation (D_{acc}–D_{plan}). Large dose deviations were also observed relative to D_{pred}, suggesting full dose accumulation (D_{acc}) may be beneficial for future SBRT trials. One patient's duodenum exceeded the planned tolerance when the maximum dose increased by 4% (D_{acc}–D_{pred}), or 0.7 Gy, not thought to be clinically significant. Research is ongoing to correlate accumulated dose with clinical outcomes. Exploiting anatomical changes with adaptive SBRT, could possibly safely allow further dose escalation. Deviations caused by uncertainties not modeled in this study include, intrafraction motion, stomach filling, and changes to the dose matrices caused by external contour variations, need to also be quantified.

Many tissues had large geometric errors exceeding the IGRT tolerance of 3 mm, yet had negligible dose changes. GTVs are buffered by the PTV and degree of surrounding dose conformality. It is also expected that sharper dose gradients are more sensitive to geometric errors causing larger dose deviations (22). For 4D CT-predicted dose distributions in the liver, larger tumor changes have been observed for IMRT versus conventional plans(10). DIR and dose accumulation can aid in evaluating the robustness of planning solutions on predicting the accumulated dose. Highly conformal techniques (i.e. IMRT) can improve target coverage, spare normal tissue and possibly allow dose-escalation on the static distribution (23), or predicted breathing distribution. Stricter IGRT tolerances are required to minimize accumulated dose deviations for more conformal plans.

Residual setup caused the majority of dose deviations. Many patients had half their SBRT course with tumor displacements (exhale CT versus exhale 4D CBCT) exceeding the IGRT tolerance. These residual setup errors are likely due to the inherent uncertainties in using the liver as a surrogate, breathing artifacts on the CBCT, and the rigid registration used. Baseline shifts in liver position relative to bony anatomy were largely accounted for through the use of CBCT and soft-tissue targeting, and thus not a significant contributor to dose deviations. Neither DIR nor 4D CBCT for online localization were available clinically during the study period.

4D CBCT has the potential to capture both baseline shifts and breathing motion even with simple rigid liver registration (12, 24). Combining online DIR with a priori motion models to improve the quality of the 4D CBCT(25), or target the tumor in with limited 2D imaging(26) may also improve IGRT. Many patients had breathing variations (4D CBCT versus 4D CT) thought they were relatively stable, as has been observed in other 4D CBCT studies of the lung and liver(12, 27). Breathing dose distributions (D_{pred}) should be implemented only if the planning 4D CT is representative of the treatment breathing motion. Case et al. (12) reported that mean 4D CBCT motion correlated well with 4D CT, though this was evaluated using rigid liver registration. Substantial geometric differences have been observed between rigid and DIR modeling of breathing motion(9).

Although deformation had less impact on D_{acc} than residual setup, this should not be interpreted that DIR can be replaced by rigid registration. DIR facilitated dose accumulation, and was used for all breathing models. In cases where large anatomical deformations are observed, and cannot be corrected for with IGRT alone (Fig. 5), re-simulation and re-planning is strongly recommended. DIR and dose accumulation may also facilitate this,

though rigorous geometric and dosimetric validation is necessary prior to clinical implementation.

Conclusions

Deformable registration of 4D CBCT and dose accumulation improved estimates of the delivered dose to targets and normal tissues in free-breathing liver SBRT patients. The majority of patients had accumulated dose deviations greater than 5% relative to the static clinical plan. Breathing dose distributions predicted with the planning 4D CT can help reduce the overall uncertainty at planning in certain normal tissues, but large deviations still occurred in nearly half the patients. Breathing dose distributions may need to be coupled with improvements in IGRT prior to clinical implementation as residual setup uncertainties commonly caused dose deivations. Full dose accumulation during SBRT can account for residual anatomical deformations, and may facilitate the development of adaptive therapy and the pursuit of further safe dose-escalation. Accumulated dose may help interpret clinical outcomes of SBRT response and toxicity.

Acknowledgments

We thank Jan-Jakob Sonke and Marcel van Herk (The Netherlands Cancer Institute) for help with the 4D cone-beam CT; Graham Wilson and Michael Sharpe for valuable assistance with this research. This work is supported by the U.S. National Institutes of Health, 5RO1CA124714-02. Clinical trials were supported by the NCIC (Grant 18207) and Elekta Oncology Systems. K. K. Brock is supported as a Cancer Care Ontario Research Chair.

References

1. Ben-Josef E, Normolle D, Ensminger WD, et al. Phase II trial of high-dose conformal radiation therapy with concurrent hepatic artery floxuridine for unresectable intrahepatic malignancies. J Clin Oncol. 2005; 23:8739–8747. [PubMed: 16314634]
2. Dawson LA, Eccles C, Craig T. Individualized image guided iso-NTCP based liver cancer SBRT. Acta Oncol. 2006; 45:856–864. [PubMed: 16982550]
3. Katz AW, Carey-Sampson M, Muhs AG, et al. Hypofractionated stereotactic body radiation therapy (SBRT) for limited hepatic metastases. Int J Radiat Oncol Biol Phys. 2007; 67:793–798. [PubMed: 17197128]
4. Lee MT, Kim JJ, Dinniwell R, et al. Phase I study of individualized stereotactic body radiotherapy of liver metastases. J Clin Oncol. 2009; 27:1585–1591. [PubMed: 19255313]
5. Tse RV, Hawkins M, Lockwood G, et al. Phase I study of individualized stereotactic body radiotherapy for hepatocellular carcinoma and intrahepatic cholangiocarcinoma. J Clin Oncol. 2008; 26:657–664. [PubMed: 18172187]
6. Hawkins MA, Brock KK, Eccles C, et al. Assessment of residual error in liver position using kV cone-beam computed tomography for liver cancer high-precision radiation therapy. Int J Radiat Oncol Biol Phys. 2006; 66:610–619. [PubMed: 16966004]
7. Wunderink W, Mendez Romero A, de Kruijf W, et al. Reduction of respiratory liver tumor motion by abdominal compression in stereotactic body frame, analyzed by tracking fiducial markers implanted in liver. Int J Radiat Oncol Biol Phys. 2008; 71:907–915. [PubMed: 18514783]
8. Rosu M, Dawson LA, Balter JM, et al. Alterations in normal liver doses due to organ motion. Int J Radiat Oncol Biol Phys. 2003; 57:1472–1479. [PubMed: 14630287]
9. Velec M, Moseley JL, Eccles CL, et al. Effect of breathing motion on radiotherapy dose accumulation in the abdomen using deformable registration. Int J Radiat Oncol Biol Phys. 2011; 80:265–272. [PubMed: 20732755]
10. Wu QJ, Thongphiew D, Wang Z, et al. The impact of respiratory motion and treatment technique on stereotactic body radiation therapy for liver cancer. Med Phys. 2008; 35:1440–1451. [PubMed: 18491539]

11. Brock KK, Hawkins M, Eccles C, et al. Improving image-guided target localization through deformable registration. Acta Oncol. 2008; 47:1279–1285. [PubMed: 18766475]
12. Case RB, Moseley DJ, Sonke JJ, et al. Interfraction and intrafraction changes in amplitude of breathing motion in stereotactic liver radiotherapy. Int J Radiat Oncol Biol Phys. 2010; 77:918–925. [PubMed: 20207501]
13. Wunderink W, Mendez Romero A, Seppenwoolde Y, et al. Potentials and limitations of guiding liver stereotactic body radiation therapy set-up on liver-implanted fiducial markers. Int J Radiat Oncol Biol Phys. 2010; 77:1573–1583. [PubMed: 20399034]
14. Guckenberger M, Sweeney RA, Wilbert J, et al. Image-guided radiotherapy for liver cancer using respiratory-correlated computed tomography and cone-beam computed tomography. Int J Radiat Oncol Biol Phys. 2008; 71:297–304. [PubMed: 18406894]
15. Mendez Romero A, Zinkstok RT, Wunderink W, et al. Stereotactic body radiation therapy for liver tumors: impact of daily setup corrections and day-to-day anatomic variations on dose in target and organs at risk. Int J Radiat Oncol Biol Phys. 2009; 75:1201–1208. [PubMed: 19386435]
16. Janssens G, de Xivry JO, Fekkes S, et al. Evaluation of nonrigid registration models for interfraction dose accumulation in radiotherapy. Med Phys. 2009; 36:4268–4276. [PubMed: 19810501]
17. Sonke JJ, Zijp L, Remeijer P, et al. Respiratory correlated cone beam CT. Med Phys. 2005; 32:1176–1186. [PubMed: 15895601]
18. Brock KK, Sharpe MB, Dawson LA, et al. Accuracy of finite element model-based multi-organ deformable image registration. Med Phys. 2005; 32:1647–1659. [PubMed: 16013724]
19. Lujan AE, Larsen EW, Balter JM, et al. A method for incorporating organ motion due to breathing into 3D dose calculations. Med Phys. 1999; 26:715–720. [PubMed: 10360531]
20. van Herk M. Errors and margins in radiotherapy. Semin Radiat Oncol. 2004; 14:52–64. [PubMed: 14752733]
21. van Mourik A, van Kranen S, den Hollander S, et al. Effects of setup errors and shape changes on breast radiotherapy. Int J Radiat Oncol Biol Phys. 2011; 79:1557–1564. [PubMed: 20933341]
22. Lim K, Kelly V, Stewart J, et al. Pelvic radiotherapy for cancer of the cervix: is what you plan actually what you deliver? Int J Radiat Oncol Biol Phys. 2009; 74:304–312. [PubMed: 19362250]
23. Eccles CL, Bissonnette JP, Craig T, et al. Treatment planning study to determine potential benefit of intensity-modulated radiotherapy versus conformal radiotherapy for unresectable hepatic malignancies. Int J Radiat Oncol Biol Phys. 2008; 72:582–588. [PubMed: 18793961]
24. Case RB, Sonke JJ, Moseley DJ, et al. Inter- and intrafraction variability in liver position in non-breath-hold stereotactic body radiotherapy. Int J Radiat Oncol Biol Phys. 2009; 75:302–308. [PubMed: 19628342]
25. Rit S, Wolthaus JW, van Herk M, et al. On-the-fly motion-compensated cone-beam CT using an a priori model of the respiratory motion. Med Phys. 2009; 36:2283–2296. [PubMed: 19610317]
26. Nguyen TN, Moseley JL, Dawson LA, et al. Adapting liver motion models using a navigator channel technique. Med Phys. 2009; 36:1061–1073. [PubMed: 19472611]
27. Sonke JJ, Lebesque J, van Herk M. Variability of four-dimensional computed tomography patient models. Int J Radiat Oncol Biol Phys. 2008; 70:590–598. [PubMed: 18037579]

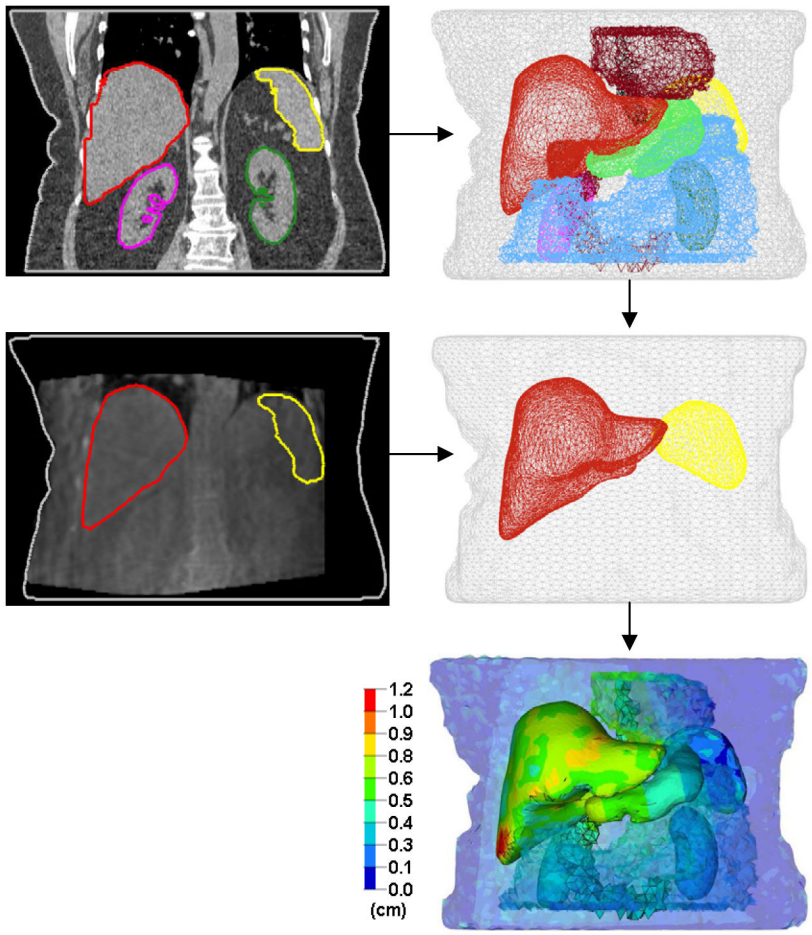

Fig. 1.
Example of multi-organ deformable registration between exhale CT (top) and exhale CBCT (middle), and the resulting deformation map (bottom).

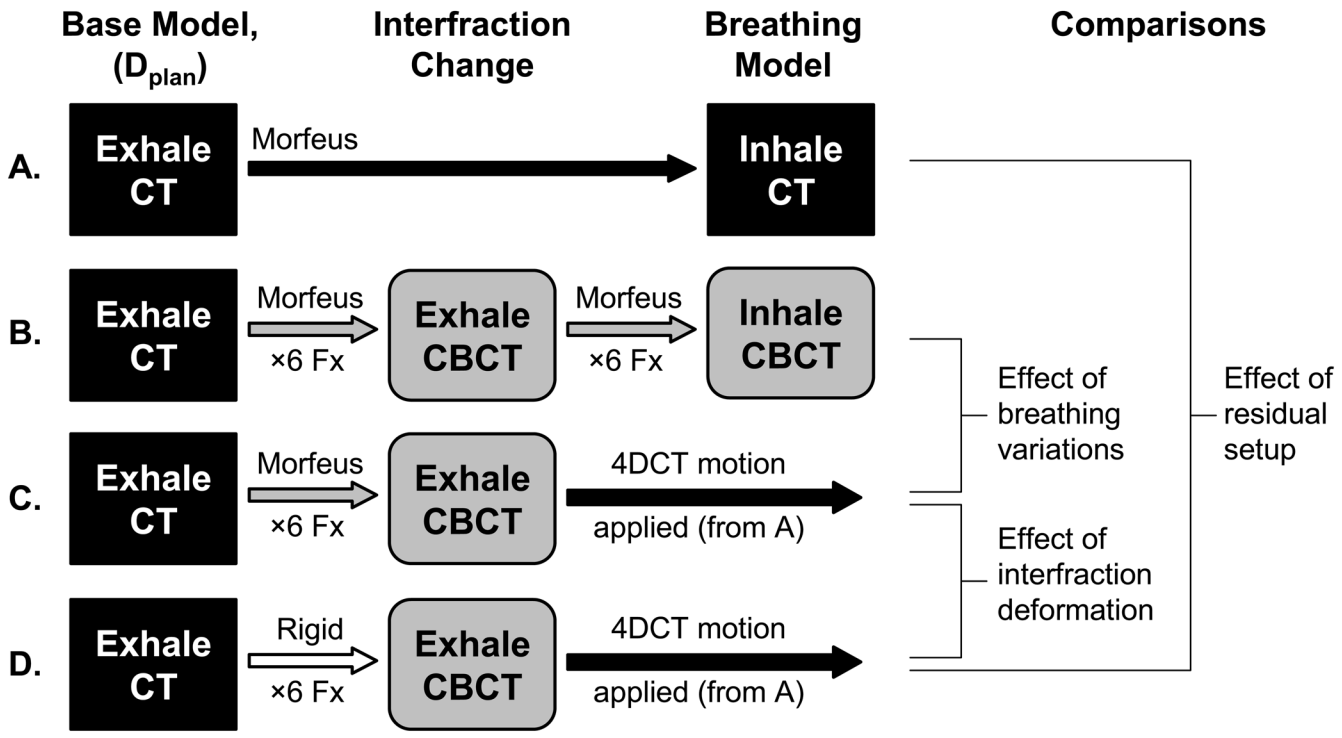

Fig. 2.

Schema of dose accumulation comparisons to extract the contribution of geometric uncertainties on dose deviations: A. predicted 4D CT breathing dose (D_{pred}); B. full SBRT dose accumulation (D_{acc}); C. deformable interfraction accumulation with the 4D CT breathing motion applied; D. rigid interfraction accumulation with the 4D CT breathing motion applied; Morfeus=deformable registration. Rigid=liver-to-liver centre-of-mass registration. Fx=fractions.

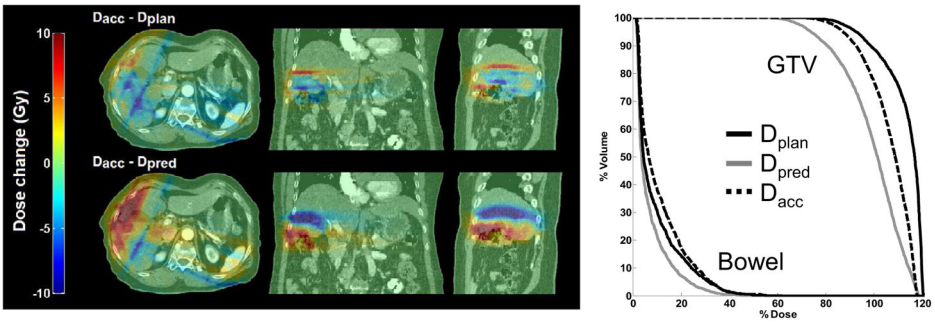

Fig 3.

Deviations from the accumulated dose (D_{acc}) are shown. PTV coverage was compromised inferiorly on the static exhale CT plan (D_{plan}) to spare the large bowel. 4D CT (D_{pred}) predicted less dose as these tissues moved inferior away from the high-dose region. Geometric errors seen on 4D CBCT moved these tissues back towards the high-dose region.

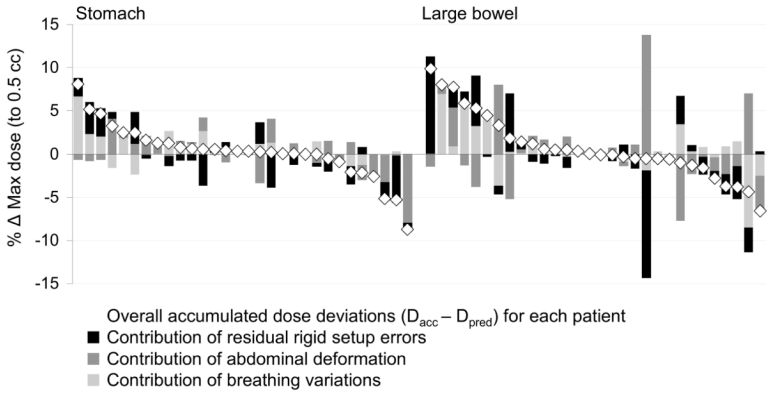

Fig 4.

The relative contribution of geometric errors to changes between the accumulated (D_{acc}) and predicted (D_{pred}) dose, for all patients' stomachs and bowels.

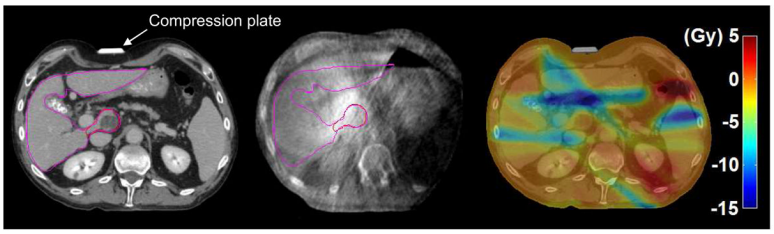

Fig 5.

An example of large dose deviations due to deformation. Left: patient was planned and on exhale CT for 30 Gy with abdominal compression (liver=purple; GTV=red). Middle: deformation in the abdomen shown on CBCT was possibly due to a misaligned compression plate and increased stomach contents. Right: differences between the accumulated and predicted dose (D_{acc}–D_{pred}) showing decreases (dark blue region) to the minimum GTV of 4.3 Gy, and the maximum duodenum by 11.5 Gy.

Table 1

Patient characteristics and SBRT treatment details.

Patients (*n*)	30
Age [median (range)] (y)	72 (45 – 83)
Gender: male/female (*n*)	19/11
Diagnosis (*n*)	
Primary liver cancer	15
Liver metastases	15
No. GTV [median (range)] (*n*)	2 (1 – 5)
GTV volume [mean (range)] (cc)	162 (4 – 707)
Motion management (*n*)	
Free-breathing	11
Abdominal compression plate	19
Planned fluoroscopy motion [mean (range)] (mm)	9 (2 – 17)
PTV [mean (max)] (mm)	
Left	6 (13)
Right	5 (7)
Anterior	7 (20)
Posterior	5 (8)
Superior	5 (6)
Inferior	12 (23)
No. beams, excluding segments [median (range)] (*n*)	6 (4 – 15)
Liver NTCP [mean (range)] (%)	1.8 (0 – 15.2)
Prescribed dose in 6 fractions [mean (range)] (Gy)	39 (27 – 60)

Abbreviations: GTV=gross tumour volumes; PTV=planning target volume; NTCP=normal tissue complication probability (biologically corrected to 2 Gy/fraction).

Table 2

Population geometric uncertainties (in mm) at planning and during 6-fraction SBRT evaluated with deformable image registration.

		Exhale CT to Inhale CT		Exhale CT to Exhale CBCT		Exhale CBCT to Inhale CBCT	
		Rigid	Deformation	Rigid	Deformation	Rigid	Deformation
		Mean, SD	SD*, RMS†	Mean, Σ_{COM}, σ_{COM}	Σ_{DEF}, σ_{DEF}	Mean, Σ_{COM}, σ_{COM}	Σ_{DEF}, σ_{DEF}
GTV	LR	−1.3, 2.1	1.0, 1.0	0.7, 1.8, 1.7	1.0, 1.2	−1.2, 1.1, 1.1	0.5, 0.4
	AP	3.7, 3.0	1.7, 0.8	−0.8, 2.2, 1.9	0.9, 1.1	2.9, 1.6, 1.5	0.6, 0.5
	SI	8.8, 5.0	1.9, 1.2	−0.5, 2.6, 2.4	1.0, 1.2	7.0, 3.1, 1.6	0.7, 0.8
Liver	LR	−1.1, 2.0	0.5, 1.5	0.5, 1.7, 1.9	0.4, 1.6	−1.2, 1.0, 1.0	0.2, 0.7
	AP	3.9, 2.3	0.4, 1.8	−0.8, 2.2, 1.9	0.4, 1.6	3.1, 1.7, 1.5	0.2, 1.0
	SI	9.0, 5.2	0.5, 2.0	−0.4, 2.1, 2.4	0.3, 1.8	7.1, 3.2, 1.4	0.2, 1.2

Abbreviations: CT=computed tomography; CBCT=cone-beam CT; COM=centre-of-mass; DEF=deformation; SD=standard deviation; RMS=root mean square; Σ=group systematic error; σ=group random error; GTV=gross tumor volumes;

Notes: Positive M values are displacements in the left, anterior, inferior directions.

*SD of each patient's mean elements' motion (minus liver COM).

†RMS of the SD of the each patient's elements' motion (minus liver COM).

Table 3

Accumulated treatment dose (D_{acc}) deviations relative to the planned static dose (D_{plan}) and the predicted 4D CT breathing dose (D_{pred}).

	Accumulated (D_{acc}) vs. planned (D_{plan})			**Accumulated (D_{acc}) vs. predicted (D_{pred})**			
	Mean, SD, in Gy	**Max, Min in Gy (% of Rx)**	**Patients with |Δ| ≥ 5%**	**Mean, SD, in Gy**	**Max, Min in Gy (% of Rx)**	**Patients with |Δ| ≥ 5%**	**D_{acc}-D_{plan} vs D_{acc}-D_{pred}**
GTV (min to 0.5 cc), n=54	−0.2, 1.0	−4.4, 2.3 (−15, 5)	10%	0.1, 1.4	−4.3, 8.1 (−14, 13)	10%	
Liver (mean), n=30	−0.2*, 0.5	−1.7, 0.9 (−6, 2)	3%	−0.1, 0.6	−1.5, 1.0 (−5, 3)	3%	
Large bowel (max to 0.5 cc), n=30	−1.1*, 1.5	−5.3, 1.3 (−15, 3)	33%	0.4, 1.7	−2.3, 5.9 (−7, 10)	20%	*
Small bowel (max to 0.5 cc), n=15	−1.3*, 2.2	−7.8, 0 (−26, 0)	20%	−0.6, 2.1	−6.5, 1.7 (−22, 5)	33%	*
Duodenum (max to 0.5 cc), n=30	−1.5*, 2.6	−12.6, 0.7 (−42, 3)	33%	−0.2, 2.5	−11.5, 5.2 (−38, 9)	7%	*
Esophagus (max to 0.5 cc), n=29	0.3*, 0.8	−0.8, 2.4 (−3, 8)	7%	−0.3, 0.9	−2.9, 2.0 (−6, 5)	14%	*
Stomach (max to 0.5 cc), n=30	−0.4, 1.5	−4.3, 4.6 (−14, 8)	17%	0, 1.2	−3.2, 2.7 (−9, 8)	20%	*
Right kidney (mean), n=30	−0.4*, 0.7	−2.0, 0.6 (−5, 2)	10%	0, 0.9	−2.0, 3.9 (−5, 7)	7%	*
Left kidney (mean), n=30	−0.1, 0.3	−1.2, 0.4 (−3, 1)	0%	0.1, 0.2	−0.7, 0.6 (−2, 2)	0%	*
Heart (max to 0.5 cc), n=25	−0.5*, 1.0	−4.0, 0.8 (−13, 2)	8%	−1.0*, 1.9	−8.2, 0.6 (−19, 2)	16%	*
	Mean, SD, in % NTCP	Max, Min, in % NTCP	Patients with |Δ| ≥ 5%	Mean, SD, in % NTCP	Max, Min, in % NTCP	Patients with |Δ| ≥ 5%	
Liver (NTCP), n=30	−0.5, 2.5	−8.3, 8.0	10%	0.6, 2.4	−2.1, 9.4	7%	

Abbreviations: SD=standard deviation; NTCP=normal tissue complication probability; GTV=gross tumour volumes.

*p<0.05 on paired t-test.